Pis'ma v ZhETF, vol. 94, iss. 11, pp. 904 – 910 

# Curvature-dependent excitation propagation in cultured cardiac tissue

*S. Kadota*[+], *M. W. Kay*[*], *N. Magome*[+], *K. Agladze*[+×1)]

[+]*Institute for Integrated Cell-Material Sciences, Kyoto University, 606-8501 Kyoto, Japan*

[*]*Department of Electrical and Computer Engineering, The George Washington University, 20052 Washington DC, USA*

[×]*Research and Education Center Bionanophysics, Moscow Institute of Physics and Technology, 141700 Dolgoprudny, Russia*

Submitted 14 October 2011

The geometry of excitation wave front may play an important role on the propagation block and spiral wave formation. The wave front which is bent over the critical value due to interaction with the obstacles may partially cease to propagate and appearing wave breaks evolve into rotating waves or reentry. This scenario may explain how reentry spontaneously originates in a heart. We studied highly curved excitation wave fronts in the cardiac tissue culture and found that in the conditions of normal, non-inhibited excitability the curvature effects do not play essential role in the propagation. Neither narrow isthmuses nor sharp corners of the obstacles, being classical objects for production of extremely curved wave front, did not affect non-inhibited wave propagation. The curvature-related phenomena of the propagation block and wave detachment from the obstacle boundary were observed only after partial suppression of the sodium channels with Lidocaine. Computer simulations confirmed the experimental observations. The explanation of the observed phenomena refers to the fact that the heart tissue is made of finite size cells so that curvature radii smaller than the cardiomyocyte size loses sense, and in non-inhibited tissue the single cell is capable to transmit excitation to its neighbors.

**1. Introduction.** Life threatening arrhythmia, such as ventricular tachycardia and fibrillation (VT/VF) is one of the leading causes of sudden cardiac death. It is generally believed that spiral-reentry is the major organization center of VT/VF [1]. Disorder of the excitation propagation may lead to circulating excitation, or reentry, a self-perpetuating mechanism involved in the initiation and maintenance of the majority of tachyarrhythmia. The geometry of excitation wave front plays an important role on the propagation block and spiral wave formation. The curvature of the propagating excitation wavefront and the interaction of the wavefront with the repolarization tail of the preceding wave are important determinant of impulse propagation [2, 3]. The wave front bent over the critical value due to interaction with the obstacles may partially cease to propagate and created wave breaks may evolve into rotating waves or reentry. In most regions of the heart propagating electric waves interact with tissue structures [4, 5]. The three most frequent studied elements of tissue geometry are: 1) a simple linear connective tissue structure with a sharp end [6, 7]; 2) a small isthmus within a connective tissue structure connecting two large regions of myocardial tissue [8, 9]; and 3) an abruptly changing tissue geometry [10, 11]. Wave propagation through the narrow isthmus structure was studied in isolated cardiac muscle [8], and it was shown that beyond the isthmus propagation of the wave is substantially slowed by the wave front curvature [8] although without quantitative data. The cultured monolayer of cardiomyocytes gives more control over the precise geometry of the conducting tissue, thus giving a simplified but helpful two-dimensional tissue model for the qualitative and quantitative studying of the arrhythmias mechanisms related to the topology and function of the cell network [12].

Our goal was to study the curvature-dependent excitation propagation in the cultured cardiac monolayers and its response to the various anti-arrhythmic drugs. The most promising conservative therapy against reentry-based arrhythmias is application of ion channel blockers, such as amiodarone or lidocaine [13]. Intravenous amiodarone is approved by Food and Drug Administration for treatment and prevention of VF and hemodynamically unstable VT [14]. Nifekalant, a selective blocker of the rapid component of the delayed rectifier $K^+$-current ($I_{Kr}$), was reported to promote self-termination of VT through destabilization of spiral waves [15]. On the other hand, it is well known that excessive prolongation of ventricular action potentials by $K^+$-channel blockers (drug-induced QT-prolongation) leads to an induction of polymorphic VT [16]. Lidocaine was also reported to be arrhythmogenic because of rate-dependent conduction velocity depression and nonuniform activation [17].

The trend of the excitation propagation patterns under Lidocaine was confirmed by the computer simulations.

[1)] e-mail: agladze@yahoo.com

**2. Methods.** This study conforms to the Guide for the Care and Use of Laboratory Animals published by the US National Institutes of Health (NIH) and was approved by the Animal Research Committee, Kyoto University.

*2.1. Culture of Neonatal Rat Cardiac Myocytes.* Primary cell cultures of neonatal rat ventricular myocytes were prepared as described elsewhere [18] Briefly, hearts were removed from 1- to 2-day-old Wistar rats (Japan SLC) anesthetized by isoflurane (Abbott). The hearts were minced and digested 2 times for 15 min each with 10 ml of PBS containing 0.2% collagenase type I (Wako). The isolated cells were collected by centrifugation and incubated in 100-mm cell culture dishes (IWAKI) for 1 h at 37 °C in a humidified incubator with 5% $CO_2$ air. After supernatant was collected again, the cells were seeded into 27-mm diameter glass plates (IWAKI) coated with fibronectin (16.7 $\mu$g/ml) at a cell density of $2.6 \cdot 10^3\,\mathrm{mm}^{-2}$. The cells were incubated in Dulbecco-modified Eagle medium supplemented with 10% fetal bovine serum and 1% penicillin streptomycin. After 24 h, the medium was replaced with minimum essential medium supplemented with 10% calf serum and 1% penicillin streptomycin, and the cells were incubated under the same condition.

*2.2. Optical Mapping System.* Excitation waves were observed 5–10 days after culturing. The medium was exchanged with Tyrode's solution (Sigma) and kept at room temperature. Cells were labeled with a $Ca^{2+}$ sensitive fluorescent dye, Fluo-4 (Invitrogen). Fluorescent light was observed by highspeed CCD camera (pco.1200hs; PCO AG) and image intensifier unit (C8600; Hamamatsu), connected to microscope (MVX10; Olympus) with 280×280 pixels at 50 fps. The microscope was equipped with zooming function ranging from the cellular level (×6.3; dimension of 2.5 mm) to the tissue level (×0.63; dimension of 25 mm). In some instances, acquired data were further processed for noise reduction by image processing system (ImageJ, NIH). Time-space plot was made by the Reslice function of ImageJ with horizontal 1 pixel at 20 ms.

*2.3. Obstacles and Drug Treatment.* Obstacles in the cardiac cell sheets were made by precise cuts in the central area of cultured monolayer with 27G syringe needle controlled by micro manipulator under the phase-contrast microscope (IX-71; Olympus), just before the observation. In order to create the narrow isthmus, the cut line was briefly interrupted by elevating the needle, leaving small non cut area in the center (fig. 1a). For the modeling of spiral wave formation on a sharp feature, one-sided line was cut (fig. 1b). In order to control the excitability and the restitution, either Lidocaine or

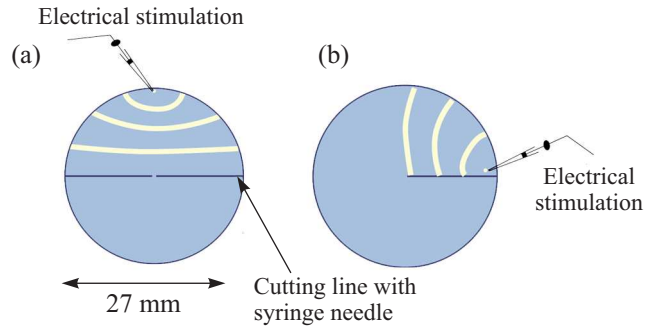


Fig. 1. (a) – Narrow isthmus model. (b) – Spiral wave formation model

Nifekalant, or the mixture of thereof were added to the incubation solution. Lidocaine was added to the final concentrations ranging from 0.2 to 1.0 mM. Nifekalant was added in concentration range from 1.0 to 10 $\mu$M.

*2.4. Experimental Protocol.* Bipolar stimulating electrode was positioned at the rim of the myocyte layers in order to minimize the damage to the studied area in the center of the layer. Trains of pulses were applied at 2.0 V and 20 ms, at least 10 s with a progressive decrease of stimulation cycle length (CL) from 1.0 s to 300 ms until the capture failure. In the case when excitation wave could not be initiated with the stimulation CL of 1 s, the stimulation CL increased until 2.0 s or the voltage of stimulation increased until 4.0 V.

*2.5. Computational model.* Wave front propagation through an isthmus was simulated using a continuous isotropic cardiac sheet model discretized on a rectangular mesh with no-flux boundary conditions [19]. The typical mesh size was $1.5 \times 1.5\,\mathrm{mm}^2$ with $dx = 5\,\mu$m. The equation governing the transmembrane potential ($V_m$, mV) at each node was

$$\frac{\partial V_m}{\partial t} = D\nabla^2 V_m - \frac{I_{\mathrm{ion}}}{C_m}, \qquad (1)$$

where $C_m$ is the membrane capacitance ($1.0\,\mu\mathrm{F}\cdot\mathrm{cm}^{-2}$), $D$ is the diffusion coefficient ($0.9\,\mathrm{cm}^2\cdot\mathrm{s}^{-1}$), $I_{\mathrm{ion}}$ is the total current flowing through the membrane ($\mu\mathrm{A}\cdot\mathrm{cm}^{-2}$), and $\nabla^2$ is the 2D-spatial Laplacian ($\mathrm{cm}^{-2}$). Equation (1) was integrated using a forward Euler method with a time step of $dt = 0.04\,\mu$s. The Laplacian was evaluated explicitly using a 9-point second difference approximation. The membrane current kinetics of $I_{\mathrm{ion}}$ are described by Hodgkin–Huxley type equations with the Drouhard–Roberge [20] formulation of the inward sodium current and the Beeler–Reuter [21] formulations of the slow inward current ($I_s$), time-independent potassium current ($I_{K1}$), and time-activated outward current ($I_{x1}$). To approximate the action potential duration of rat neonatal myocytes the time constants of $Ca^{2+}$ cur-

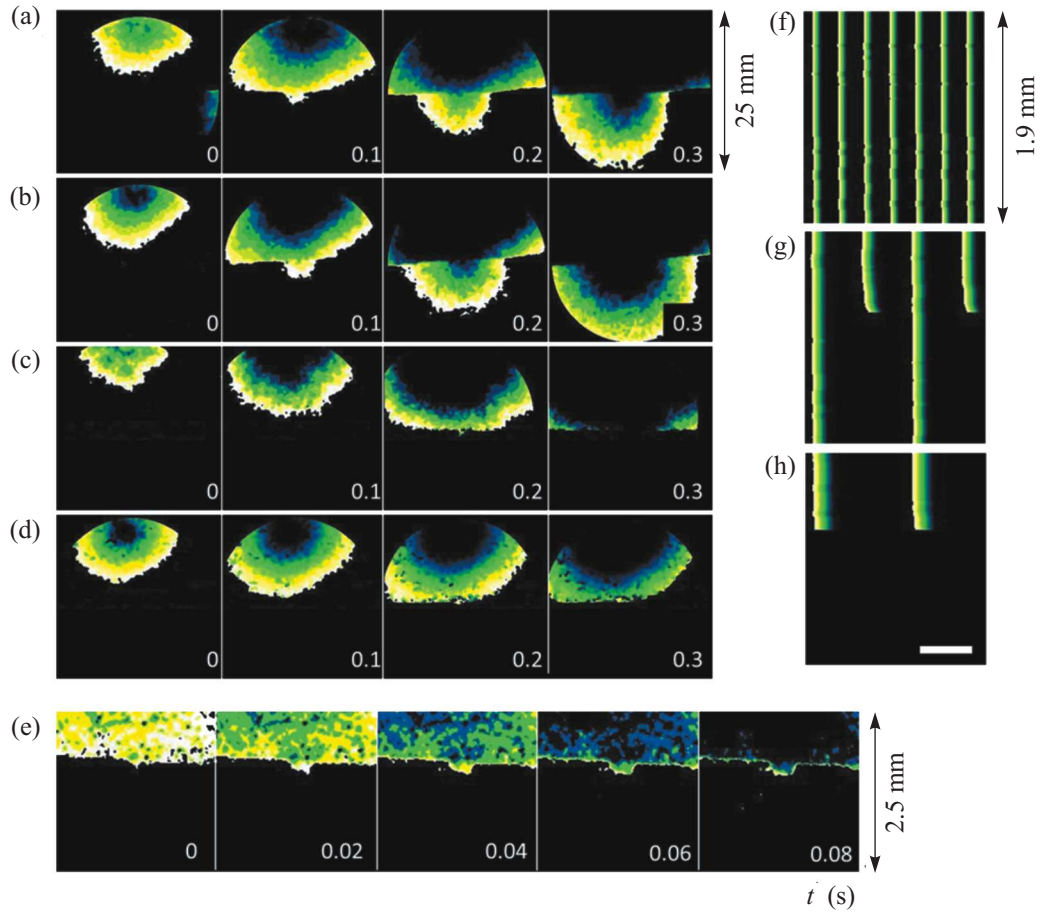


Fig. 2. Propagation pattern through the narrow isthmus on the cultured cardic tissue. (f)–(h) – Time-space plot of the wave propagation beyond the isthmus. Experimental parameters are followings: 97 $\mu$m width, Lidocaine 0.2 mM, stimulation CL 0.6 s (a); 97 $\mu$m width, Lidocaine 0.2 mM, Nifekalant 10 $\mu$m, stimulation CL 0.6 s (b); 97 $\mu$m width, Lidocaine 0.5 mM, stimulation CL 2.0 s (c); 97 $\mu$m width, Lidocaine 0.5 mM, Nifekalant 10 $\mu$m, stimulation CL 2.0 s (d); 108 $\mu$m width, Lidocaine 0.5 mM, stimulation CL 1.0 s (e) and (g); 108 $\mu$m width, Lidocaine (–), stimulation CL 0.5 s (f); 108 $\mu$m width, Lidocaine 1.0 mM, stimulation CL 2.0 s (h). Time interval of images are 0.1 s in (a)–(d) and 0.02 s in (e). (a) and (b) – Passing through the isthmus, but (c) and (d) – the propagation block. High magnification of the propagation block is shown in (e). (f) – passing through the isthmus. (g) – 2:1 block. (h) – The complete counduction block. Scale bar in (h) indicates 1.0 s

rent activation and inactivation were multiplied by a factor $\sigma = 0.25$ [22]. The sodium current conductance ($g$Na) was varied between 3.0 and 5.25 mS·cm$^{-2}$ to simulate changes in excitability.

An isthmus having a specific width (range: 25 to 130 $\mu$m) was established as the distance between two horizontal lines having no-flux boundary conditions that extended toward the center of the mesh (see fig. 5). Spatial and temporal discretization intervals were reduced for isthmus widths less than 30 $\mu$m to ensure numerical stability. Current injected at the bottom edge of the mesh produced planar waves that propagated toward the isthmus (fig. 5). For each value of $g$Na isthmus widths were reduced by 5 $\mu$m until the wave front failed to propagate through the isthmus. The critical isthmus width was defined as the smallest width that did not result in propagation failure.

**3. Results.**

*3.1. Propagation of excitation waves in the cultured cardiomyocytes beyond the narrow isthmus.* Our results show that, as expected, excitation propagation slowed down beyond the isthmus, fig. 2. Three major factors defined the propagation pattern beyond the isthmus: 1) the width of the isthmus; 2) concentration of Lidocaine; 3) the cycle length of the stimulation. The slowing down at the isthmus was more pronounced for the narrower isthmuses and for the larger concentrations of Lidocaine, up to a complete conduction block. Close to the conduction block it was possible to observe a rhythm transformation, when only every other or every

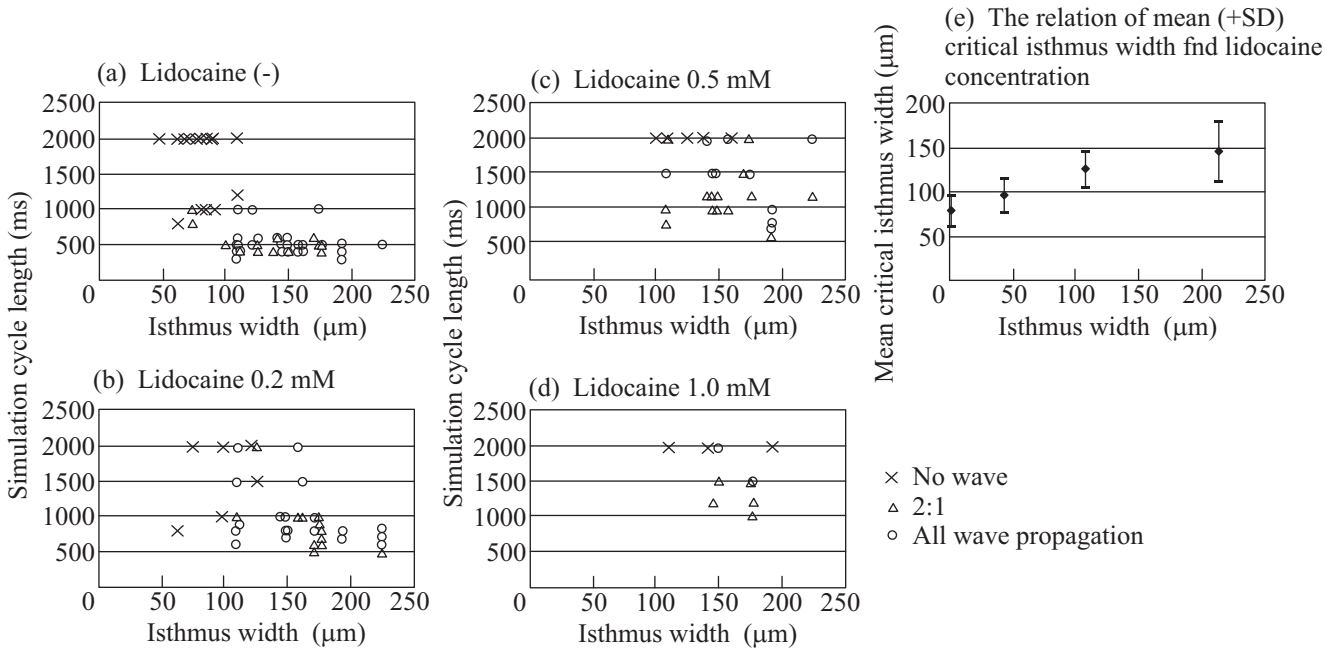


Fig. 3. The relation between the stimulation cycle length and istmus width in the experimental model. Lidocaine concentrations are 0, 0.2, 0.5, and 1.0 mM in (a), (b), (c), and (d), respectively. The mean critical isthmus width is dependent on lidocaine concentration ($n = 28$, One-way ANOVA $P = 0.002$)

third wave could pass the isthmus. Three different observed scenarios are illustrated in fig. 2f–h: a) passing the isthmus; b) rhythm transformation, c) conduction block. The time-space plots were build along the scan line drown perpendicularly through the isthmus. The tilt angle of the white line, representing the positions of the wave front on the time-space plot reflects the propagation speed, slowing down is seen as less steep tilt angle. In the absence of Lidocaine the waves successfully passed 100 $\mu$m isthmuses with no visible slowing down, fig. 2f. The application of Lidocaine allowed to observe transformation of rhythm, fig. 2g, and for larger concentrations complete conduction block, fig. 2h. For the latter cases, slowing down of the wave was visible and especially pronounced just before the propagation failure. Figure 4 shows relation between the stimulation cycle length (CL) and the gate width were made at the concentrations of Lidocaine at 0, 0.2, 0.5, and 1.0 mM, respectively. As expected, the conduction block was observed at wider isthmuses with the increase of Lidocaine concentrations. A relatively high variability may be associated with the boundary conditions of the cut; the size of the single cardiomyocyte is about 30 $\mu$m, it makes difficult expecting higher precision when removing cells from the layer by cutting them. As it is shown in fig. 4e, the mean critical isthmus width for the penetration irrespective to the stimulation frequency was 79.6, 97.7, 126.6, and 146.7 $\mu$m, for the concentration of Lidocaine 0, 0.2, 0.5, and 1.0 mM, respectively ($n = 28$, One-way ANOVA $P = 0.002$). By application of potassium channel blocker Nifekalant (up to 10 $\mu$M) without Lidocaine the wave speed and the propagation pattern didn't change. With the simultaneous application of Lidocaine and Nifekalant wave speed slightly slowed down, but the critical isthmus size did not change within the applied concentrations range, up to 10 $\mu$M, fig. 3d.

*3.2. Wave detachment from sharp edge of the obstacle.* Without application of Lidocaine, the wave detachment from the sharp edge of the obstacle was not observed, irrespective to the stimulation frequency (fig. 4a). However, if the Lidocaine was appled in concentrations exceeding 0.5 mM it was possible to observe wave detachment at the stimulation frequencies higher than 1.2 Hz, fig. 4b. Application of Nifekalant up to 10 $\mu$M, did not lead propagating wave to detach. Combined application of Nifekalant and Lidocaine, could result in the detachment of the propagating wave from the sharp edge, fig. 4c. After the detachment, two possible outcomes were observed: the waves could either rotate stably forming spiral reentry, or could migrate and disappear.

*3.3.Numerical simulations.* Computer simulations showed that depending on the isthmus size the propagation pattern changed from complete block, occasional block to continual propagation as the gate width. Figure 5a illustrates the successful propagation of the wave through the isthmus, while fig. 5b demonstrates isthmus-

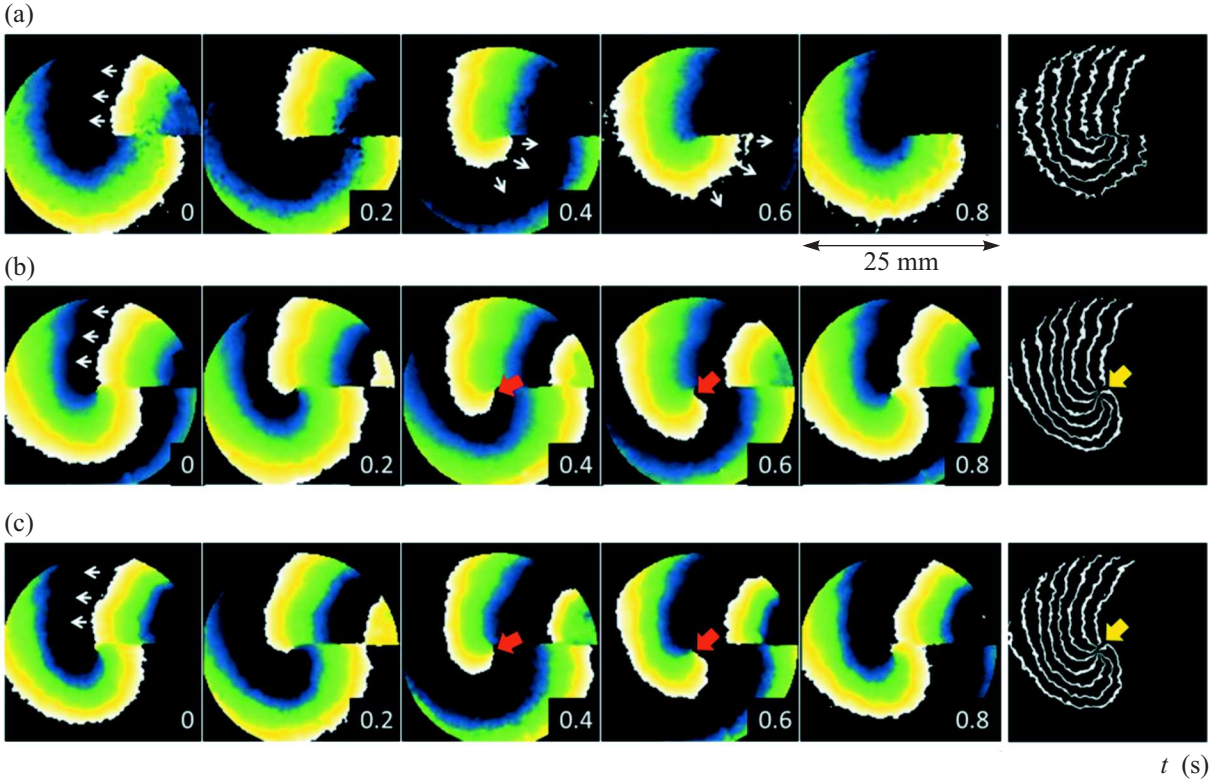


Fig. 4. Detachment from the sharp edge of obstacle for spiral wave formation. Experimental parameters are following: Lidocaine 1.0 mM, Stimulation CL 0.9 s (a), Lidocaine 1.0 mM, Stimulation CL 0.8 s (b), and Lidocaine 1.0 mM, Nifekalant 10 $\mu$M, Stimulation CL 0.8 s (c). White arrows indicate direction of the wave propagation. Red arrows in the middle of (b) and (c) indicate detachment from the sharp edge of obstacles. Right ends of each series show isochronal maps of wave front, in which line intervals are 0.1 s. Yellow arrows indicate spiral wave formations

induced block of propagation. The critical size of the isthmus for the wave to pass strongly dependent on the $g$Na, as one can see from the Fig. 6. It is important to mention that when isthmus size decreases to 20–25 $\mu$m, the further decrease does not make sense since the size of single cardiomyocyte is about this value. It means, that even single cell being excited, is able to transmit excitation to its neighbors, and the propagation block can be actually observed in the tissue with substantially decreased excitability. These data are in accordance with our experimental observations, where we could not observe the propagation block on the isthmus without application of Lidocaine.

Computer simulations also revealed an interesting fact, that isthmus can influence the propagation pattern in a way that it may exhibit early after depolarizations, fig. 7. The emergence of such depolarizations may result in reflected wave propagation. Although, we did not observe such phenomenon in our experiments, the reason might because of the relatively narrow range of the parameters allowing such wave reflection.

**4. Discussion.** Spontaneous breakup of the propagating excitation fronts is believed to be responsible for the reentry origination. Curvature of the propagating front affects its propagation speed, according to the Eiconal equation and if higher than critical, leads to the propagation failure. Of course, this approach is only valid if the propagation happens in the continuous medium, or in other words, the characteristic size of the excitable element of the medium is substantially smaller than the radius of curvature. The development of the optical mapping in the cardiac tissue called for the testing of this scenario in the real tissue. Thus, Cabo et al., 1994, in experiments with the narrow isthmus cut in the sheep heart slab, demonstrated diffraction of the planar excitation wave to the elliptical shape and showed conduction block and rhythm transform when stimulation frequency was high enough [8, 9]. The isthmuses in their experiments were of the order of 1 mm width 1 mm, thus far exceeding the size of the single cell. On the other hand, in the experiments with cardiac tissue culture, Fast et al., 1997, found unidirectional block in a

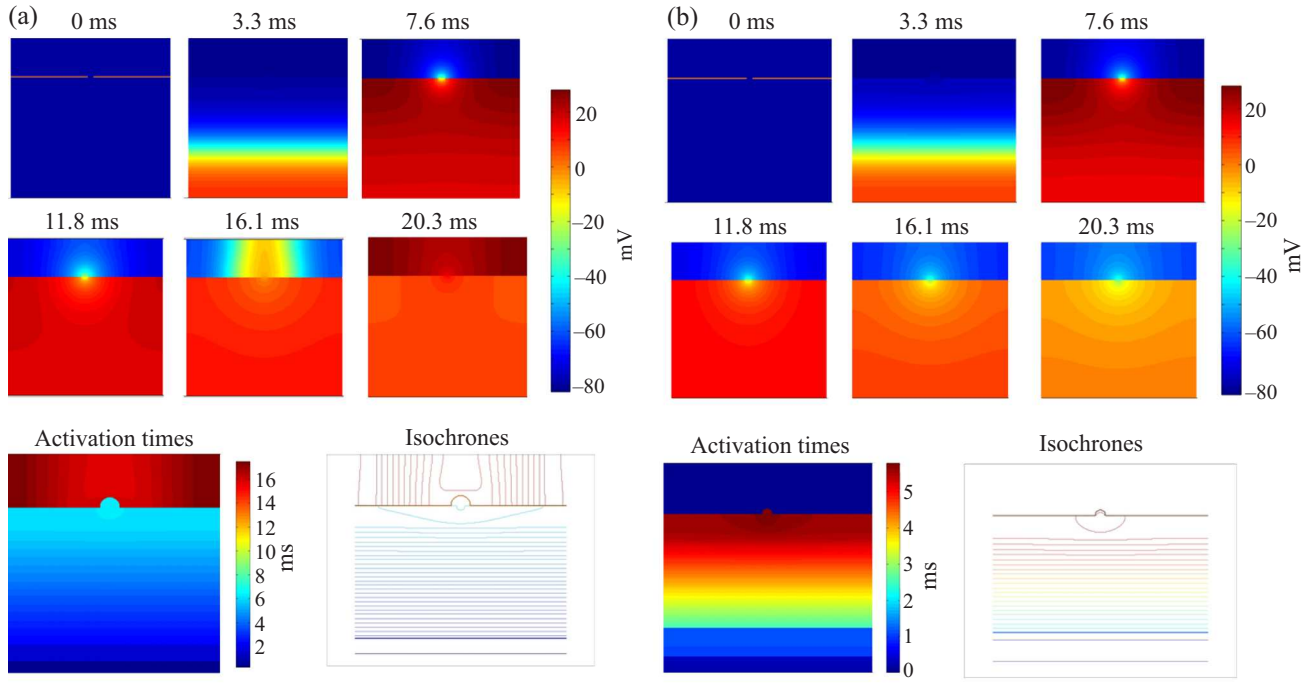


Fig. 5. (a) – Computer simulation of the propagation through the isthmus. (b) – Conduction bloc in a model of isthmus

strand of cells suddenly opening to the large area, when the width of the strand was smaller than 55 $\mu$m, which in fact, is already very close to the size of the single cardiac cell [2].

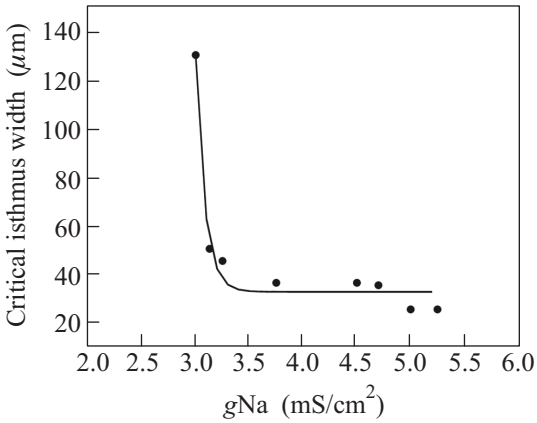


Fig. 6. Dependence of the critical isthmus size on the gNa

Surprisingly, in our experiments we could not observe the curvature-affected wave propagation in the tissue culture with normal excitability. In the normal conditions, the isthmuses with the width close to the size of the single cell did not show block of excitation propagation. Likewise, we could not observe detachment of the waves bypassing the obstacles with the sharp corners. However, curvature-related effects were observed after

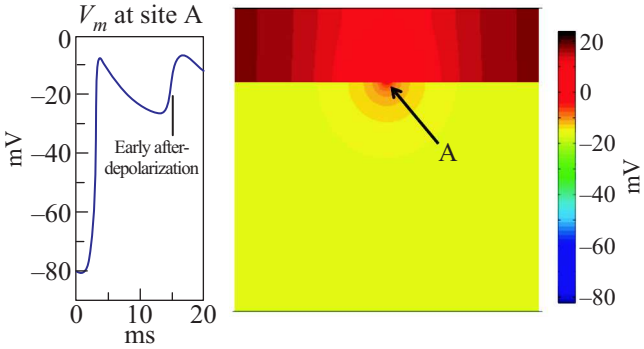


Fig. 7. Isthmus-induced early after depolarizations

application of Lidocaine, sodium channel blocker. Computer simulations also showed curvature-related slowing down at the isthmus, as well as conduction block when $g$Na was decreased about twice compare to the normal level. Surprisingly, it means that the application of the antiarrhythmic drug may in fact provoke the conduction block and reentry formation.

**5. Conclusion.** Experiments in the tissue culture demonstrated that curvature-related conduction block and spiral wave origination are observed in the tissue with substantially suppressed excitability (i.e., sodium channel activity). Otherwise, in the non-inhibited cardiac tissue the scale at which curvature of the wave front may affect propagation becomes of the order of the cell size, thus making classical continuous medium approach

inappropriate, and evidencing that even single cell is capable of transmitting excitation to its neighbors.

The authors thank Prof. A. Perzov, SUNY Upstate Medical University, and Dr. I. Motoike, Tohoku Univ., for their helpful discussions. This work is partially supported by KAKENHI-21340120 (Japan Society for the Promotion of Sciences).

1. J. M. Davidenko, A. V. Pertsov, R. Salomonsz et al., Nature **355**(6358), 349 (1992).
2. V. G. Fast and A. G. Kleber, Cardiovasc. Res. **33**(2), 258 (1997).
3. A. G. Kleber and Y. Rudy, Phys. Rev. **84**(2), 431 (2004).
4. M. S. Spach and J. M. Kootsey, Am J. Phys. Heart Circ. Phys. **244**(1), H3 (1983).
5. E. D. Overholt, R. W. Joyner, R. D. Veenstra et al., Am J. Phys. Heart Circ. Phys. **247**(4), H584 (1984).
6. S. M. Dillon, M. A. Allessie, P. C. Ursell, and A. L. Wit, Circ. Res. **63**(1), 182 (1988).
7. M. J. Schalij, W. Lammers, P. L. Rensma, and M. A. Allessie, Am J. Phys. Heart Circ. Phys. **263**(5), H1466 (1992).
8. C. Cabo, A. M. Pertsov, W. T. Baxter et al., Circ. Res. **75**(6), 1014 (1994).
9. C. Cabo, A. M. Pertsov, J. M. Davidenko et al, Biophys. J **70**(3), 1105 (1996).
10. V. G. Fast and A. G. Kleber, Cardiovasc. Res. **30**(3), 449 (1995).
11. V. G. Fast and A. G. Kleber, Cardiovasc. Res. **29**(5), 697 (1995).
12. S. Iravanian, Y. Nabutovsky, C. R. Kong et al., Am J. Phys. Heart Circ. Phys. **285**(1), H449 (2003).
13. D. P. Zipes, A. J. Camm, M. Borggrefe et al., Circulation **114**(10), e385 (2006).
14. D. Darbar, *Standard Antiarrhythmic Drugs*, In: *Cardiac Electrophysiology: From Cell to Bedside*, Fifth Edition (eds. D. P. Zipes and J. Jalife), WB Saunders, Philadelphia, 2009, p. 959.
15. M. Yamazaki, H. Honjo, H. Nakagawa et al., Am J. Phys. Heart Circ. Phys. **292**(1), H539-48 (2007).
16. D. M. Roden, N. Engl. J. Med. **350**(10), 1013 (2004).
17. K. P. Anderson, R. Walker, R. L. Lux et al., Circulation **81**(3), 1024 (1990).
18. A. Isomura, M. Horning, K. Agladze, and K. Yoshikawa, Phys. Rev. E **78**(6), 066216 (2008).
19. M. W. Kay and R. A. Gray, IEEE Trans Biomed Eng. **52**, 50 (2005).
20. J. P. Drouhard and F. A. Roberge, Comput Biomed. Res. **20**, 333 (1987).
21. G. W. Beeler and H. Reuter, J. Phys. **268**, 177 (1977).
22. K. Agladze, M. W. Kay, V. Krinsky, and N. Sarvazyan, Am. J. Phys. Heart Circ. Phys. **293**, H503 (2007).